Langmuir

Article

pubs.acs.org/Langmuir

Janus Nanoparticles as Versatile Phase-Transfer Reagents

Yang Song and Shaowei Chen*

Department of Chemistry and Biochemistry, University of California, 1156 High Street, Santa Cruz, California 95064, United States

ABSTRACT: Janus nanoparticles were prepared by interfacial ligand-exchange reactions of hexanethiolate-protected gold (AuC6) nanoparticles with 3-mercapto-1,2-propanediol (MPD) at the air|water interface. As nanoscale analogues to conventional amphiphilic molecules, the resulting Janus nanoparticles were found to form oil-in-water micelle-like or water-in-oil reverse micelle-like superparticulate structures depending on the solvent media. These unique characteristics were exploited for the effective transfer of diverse guest nanoparticles between organic and water phases. The transfer of hydrophobic nanoparticles from organic to water media or water-soluble nanoparticles to the organic phase was evidenced by transmission electron microscopy, dynamic light scattering, UV−vis, and photoluminescence measurements. In particular, line scans based on energy-dispersive X-ray analysis showed that the vesiclelike structures consisted of multiple layers of Janus nanoparticles which encapsulated the guest nanoparticles in the cores. The results highlight the unique effectiveness of using Janus nanoparticles in the formation of functional nanocomposites.

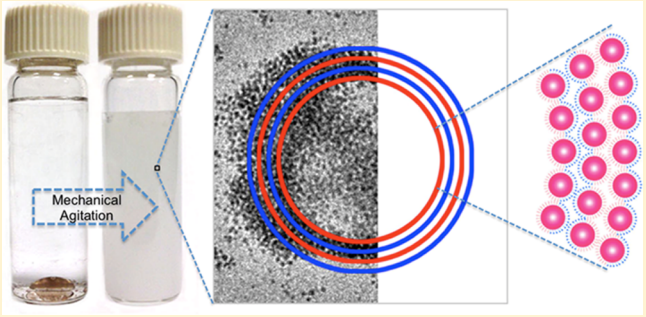

INTRODUCTION

Janus nanoparticles (JNPs), named after the two-faced Roman god Janus, refer to a unique class of nanoparticles that exhibit an asymmetrical structure including, for instance, two hemispheres of different shapes, chemical compositions, and/or surface functionality.[1] Research on these unique nanomaterials has been attracting considerable attention because of their anisotropic chemical, optical, electronic, and magnetic properties.[2−10] For organically capped nanoparticles, research on Janus nanoparticles is mostly focused on those with two kinds of organic ligands segregated on the nanoparticle surface forming a hydrophobic hemisphere and a hydrophilic one.[11−16] Recently, we developed an effective procedure based on interfacial engineering to prepare nanosized Janus particles.[17] Experimentally, a monolayer of hydrophobic alkanethiolate-protected gold nanoparticles is formed at the air|water interface by using a Langmuir−Blodgett trough. Hydrophilic thiol ligands are then injected into the water subphase to initiate ligand-exchange reactions, which are confined to the bottom face of the nanoparticles, leading to the generation of Janus nanoparticles.[17] The amphiphilic structures have been confirmed on multiple length scales, ranging from contact angle measurements of nanoparticle ensembles to adhesion force studies of individual nanoparticles and even to 2D NMR studies based on nuclear Overhauser effect spectroscopy (NOESY) of the spin interactions between neighboring molecular ligands on the nanoparticle surface.[18−21]

With their amphiphilic character, the resulting Janus nanoparticles behave as nanoscale analogues to conventional surfactant molecules. In fact, in prior studies we have shown that Janus nanoparticles may be dispersed both in water and organic media, forming stable (reverse) micelle-like aggregates.[17,22] Another unique property of amphiphilic surfactants is that they may be used as effective phase-transfer catalysts.[23−25] Thus, an immediate question arises: Will it be possible to use Janus nanoparticles as phase-transfer reagents as well? This will be of significance in the preparation and engineering of diverse functional nanocomposites. Yet, studies along this line are relatively scarce. This is the primary motivation of the present study.

Herein, we carried out a detailed study to examine the phase-transfer properties of Janus nanoparticles. The Janus nanoparticles were prepared by the interfacial ligand-exchange reaction of hydrophobic 1-hexanethiolate-protected gold nanoparticles with hydrophilic 1,2-mercapto-3-propanediol.[17] Organically soluble 1-hexanethiolate-protected silver nanoparticles and fullerene (C_{60}) were used as examples in the phase transfer from organic to aqueous media catalyzed by the Janus nanoparticles, whereas water-soluble glutathione-protected silver nanoparticles and photoluminescent carbon nanoparticles were used in the phase transfer from water to an organic phase. A variety of experimental tools were used in the structural characterization, including transmission electron microscopy, dynamic light scattering, UV−vis absorption, and photoluminescence spectroscopy. The results highlight the effectiveness of amphiphilic Janus nanoparticles in the phase transfer of diverse nanoparticle materials.

Received: March 26, 2014
Revised: May 7, 2014
Published: May 19, 2014

dx.doi.org/10.1021/la5011506 | *Langmuir* 2014, 30, 6389−6397

EXPERIMENTAL SECTION

Chemicals. Hydrogen tetrachloroauric acid ($HAuCl_4{\cdot}xH_2O$) was synthesized by dissolving ultra-high-purity gold (99.999%, Johnson Matthey) in freshly prepared aqua regia followed by crystallization.[26] Silver nitrate ($AgNO_3$, Strem, 99.9%), L-glutathione (GSH, Aldrich, 98%), tetra-*n*-octylammonium bromide (TOABr, Alfa Aesar, 98%), 1-hexanethiol (C6SH, Acros, 96%), 3-mercaptopropane-1,2-diol (MPD, Aldrich, 95%), sodium borohydride ($NaBH_4$, Acros, 99%), and fullerene (C_{60}, Acros, 99.9%) were all used as received. Solvents were purchased from typical commercial sources at their highest purities and used without further treatment. Water was supplied by a Barnstead Nanopure water system (18.3 MΩ·cm).

Hexanethiolate-Protected Gold (AuC6) and Silver (AgC6) Nanoparticles. Hexanethiolate-protected gold (AuC6) and silver (AgC6) nanoparticles were synthesized by using the Brust protocol.[27] Experimentally, 30 mL of an aqueous $AgNO_3$ or $HAuCl_4$ solution (0.03 M) was mixed with 20 mL of a toluene solution of TOABr (0.20 M) and stirred vigorously for 1 h. The organic phase was collected, into which 150 μL of 1-hexanethiol was added with a Hamilton microliter syringe. After the solution was stirred for 15 min, 24 mL of a freshly prepared ice-cold aqueous solution of 0.43 M $NaBH_4$ was added dropwise, and an immediate color change to dark brown indicated the formation of metal nanoparticles. The reaction mixtures were then stirred for 4 h to reduce the core-size dispersity before the organic phase was collected and washed five times with methanol to remove the phase-transfer catalysts, excessive 1-hexanethiol, and reaction byproducts. The average core sizes of the AuC6 and AgC6 nanoparticles were 5.0 ± 0.5 nm[22] and 5.6 ± 0.7 nm,[28,29] respectively, as determined by transmission electron microscopy measurements.

Glutathione-Protected Silver (AgGSH) Nanoparticles. Water-soluble AgGSH nanoparticles were synthesized by adopting a literature method.[30] Briefly, 0.25 mmol (42.4 mg) of $AgNO_3$ was dissolved in 50 mL of water, into which was added 1 mmol (307 mg) of GSH. A cloudy white liquid was produced due to the formation of a silver thiolate suspension, into which was then added a 10 mL aqueous solution of 0.2 M $NaBH_4$ (2.0 mmol) in a dropwise fashion under magnetic stirring. The color of the solution immediately changed from cloudy white to slightly yellow and then to dark brown in about 15 min. The reaction mixture was concentrated to a volume of ca. 5 mL in a rotary evaporator at room temperature, and AgGSH nanoparticles were precipitated by adding ∼20 mL of methanol to the solution. The precipitates were washed with methanol several times to remove excess glutathione ligands and other unreacted materials. The purified AgGSH nanoparticles were soluble in water with an average core size of ca. 1.5 nm.[30]

Carbon Nanoparticles (CNPs). The preparation of carbon nanoparticles has been detailed previously.[31,32] Briefly, 100 mg of carbon soot from the incomplete combustion of natural gas was refluxed in 10 mL of 5 M HNO_3 for 12 h. The brownish yellow supernatant after centrifugation was neutralized by Na_2CO_3 and then dialyzed against Nanopure water through a dialysis membrane for 3 days, affording purified carbon nanoparticles which exhibited an average core diameter of 4.8 ± 0.6 nm.[31,32]

Gold Janus Nanoparticles. AuC6-MPD Janus nanoparticles were prepared by using an interfacial engineering approach based on the Langmuir method, which was detailed previously.[17] Briefly, a monolayer of AuC6 nanoparticles was first deposited onto the water surface of a Langmuir–Blodgett trough (NIMA Technology, model 611D). The particle monolayer was then compressed to a desired surface pressure where the interparticle edge-to-edge separation was maintained at a value smaller than twice the extended ligand chain length such that the interfacial mobility of the particles was impeded. At this point, a calculated amount of MPD ligands was injected into the water subphase by a Hamilton microliter syringe so that interfacial ligand exchange reactions occurred. The resulting particles exhibited hydrophobic character on one face and hydrophilic on the other. The amphiphilic characters of the Janus nanoparticles were quantified by contact angle measurements (Tantec CAM-PLUS contact angle meter), where the nanoparticle monolayers were transferred onto a clean glass slide surface by either the upstroke or downstroke deposition method. The contact angles were estimated to be 86.4 ± 3.7° and 43.4 ± 4.2° for the hydrophobic and hydrophilic faces of the nanoparticles, respectively; and NMR measurements showed that the molar ratio between the two types of organic capping ligands was close to 1:1, as reported previously.[17]

Phase Transfer by Janus Nanoparticles. Phase transfers facilitated by Janus nanoparticles were tested both from CH_2Cl_2 to water and from water to CH_2Cl_2. In the transfer from CH_2Cl_2 to water, 0.05 mg of AuC6-MPD Janus nanoparticles in 300 μL of CH_2Cl_2 was added to 5 mL of water in a 7 mL glass vial, corresponding to an oil/water (o/w) ratio of 0.06:1. The vial was then subjected to mechanical agitation with a Fisher Vortex Genie 2 at approximately 3200 rpm for 10 min, after which the solution was allowed to settle down for at least 1 h. The transfer from water to CH_2Cl_2 was tested in a similar fashion. Briefly, 300 μL of water was added to a 5 mL CH_2Cl_2 solution of 0.05 mg AuC6-MPD Janus nanoparticles in a glass vial (o/w ratio 1:0.06), which was then subjected to mechanical agitation for 10 min followed by 1 h of settlement. As a control, AuC6 nanoparticles were used instead of AuC6-MPD Janus nanoparticles, and the rest of the procedure was identical.

For nanoparticle-transfer tests, the procedure was identical as well except that hydrophobic nanoparticles (AgC6 nanoparticles or C_{60}, 0.05 mg) were dispersed in 300 μL of CH_2Cl_2 and added to 0.05 mg of AuC6-MPD Janus nanoparticles in 5 mL of water or hydrophilic nanoparticles (AgGSH nanoparticles or CNPs, 0.05 mg) were dispersed in 300 μL of water and added to 0.05 mg of AuC6-MPD Janus nanoparticles in 5 mL of CH_2Cl_2.

In these studies, the nanoparticles were initially dispersed in an appropriate solvent at a concentration of ca. 0.40 mg/mL. A calculated volume (125 μL) was then transferred with a Hamilton microliter syringe to produce 0.05 mg.

Characterization. Contact angles of monolayers of the AuC6-MPD Janus nanoparticles were measured with a Tantec CAM-PLUS contact angle meter. For each sample, at least eight independent measurements were carried out for statistical analyses. UV–vis absorption spectra were collected with a Unicam ATI UV4 spectrometer by using a 1 cm quartz cuvette. The same solutions were also used for photoluminescence measurements which were carried out with a PTI fluorescence spectrometer. The morphology and sizes of the nanoparticle aggregates were characterized by transmission electron microscopic studies (TEM, Philips CM200 at 200 kV) where elemental analysis was carried out by energy-dispersive X-ray (EDX) spectroscopic measurements. Dynamic light scattering (DLS) studies were carried out by using a Wyatt DynaPro NanoStar temperature-controlled microsampler with the nanoparticles dissolved in varied solvent media. An aliquot (5 μL) of the particle solutions at a concentration of ca. 0.05 mg/mL was introduced into a sample holder by using a 10 μL micropipet. The results were reported in terms of mass %.

RESULTS AND DISCUSSION

Amphiphilicity of Janus Nanoparticles. We first tested the formation of oil-in-water micelle-like structures with AuC6-MPD Janus nanoparticles in a small amount of CH_2Cl_2 followed by the addition of a large excess of water. Experimentally, 0.05 mg of Janus nanoparticles was initially dispersed in 300 μL of CH_2Cl_2. After the addition of a large excess (5 mL) of water (o/w ratio 0.06:1), mechanical agitation led to the appearance of a rather uniform reddish solution, as depicted in Figure 1A, suggesting the homogeneous mixing of the CH_2Cl_2 and water phases. It should be noted that the solution remained stable without apparent phase separation for more than 3 days. This is in sharp contrast to only pure solvents of (5 mL) water and (300 μL) CH_2Cl_2 which are immiscible even after extensive mechanical agitation (panel B). Markedly different behaviors are also observed with AuC6

dx.doi.org/10.1021/la5011506 | Langmuir 2014, 30, 6389–6397

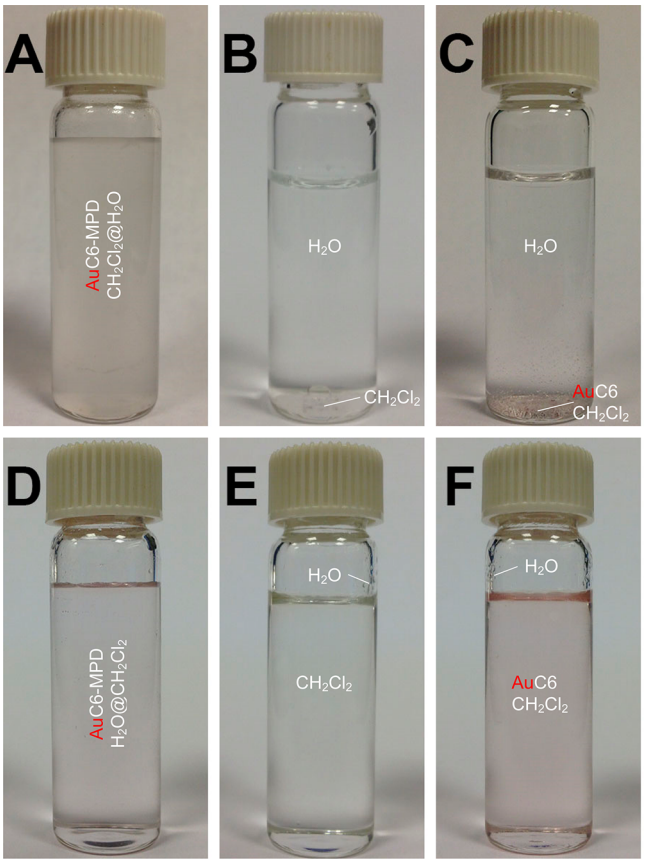

Figure 1. Photographs of solutions after mechanical agitation: (A) 0.05 mg of AuC6-MPD JNPs in 300 μL of CH_2Cl_2 with 5 mL of water; (B) 300 μL of CH_2Cl_2 with 5 mL of water; (C) 0.05 mg of AuC6 NPs in 300 μL of CH_2Cl_2 with 5 mL of water; (D) 300 μL of water with 0.05 mg of AuC6-MPD JNPs in 5 mL of CH_2Cl_2; (E) 300 μL of water with 5 mL of CH_2Cl_2; (F) 300 μL of water with 0.05 mg of AuC6 NPs in 5 mL of CH_2Cl_2.

Table 1. Average Hydrodynamic Diameters (d, nm) of Nanoparticle Ensembles in Various Media Determined by DLS Measurements

	AuC6-MPD	AuC6-MPD + AgC6	AuC6-MPD + C_{60}	AuC6-MPD + AgGSH	AuC6-MPD + CNP
CH_2Cl_2	58.2				
CH_2Cl_2–H_2O (1:0.06)	148.4			279.9	426.3
CH_2Cl_2–H_2O (0.06:1)	302.8	179.9	274.5		

nanoparticles. When 5 mL of water was added to the solution of AuC6 nanoparticles in 300 μL of CH_2Cl_2, after mechanical agitation the water phase remained clear, and at the bottom of the vial, dark-brown droplets can be found, which were the AuC6 nanoparticles in CH_2Cl_2 (note that the density of CH_2Cl_2 is higher than that of water, so the CH_2Cl_2 phase is at the bottom), as depicted in panel C.

We also tested the possibility of forming water-in-oil reverse micelle-like structures with the same Janus nanoparticles. In a similar fashion, the same quantity of Janus nanoparticles (0.05 mg) was dispersed in a large excess (5 mL) of CH_2Cl_2 and then a small amount (300 μL) of water was added (at an o/w ratio of 1:0.06), and mechanical agitation also led to the formation of a homogeneous solution, as manifested in panel D, again in sharp contrast to the case with the same amounts of (5 mL) CH_2Cl_2 and (300 μL) water only but without the Janus nanoparticles where water droplets could be clearly seen on the side of the vial (panel E) because of their immiscibility. Furthermore, solvents (5 mL) CH_2Cl_2 and (300 μL) water were not miscible with AuC6 nanoparticles dispersed in CH_2Cl_2, as manifested in panel F, where after mechanical agitation water formed droplets on the upper side of the vial.

The hydrodynamic diameters of the aggregate structures formed by the Janus nanoparticles in these different solvents were then evaluated by DLS measurements. When AuC6-MPD Janus nanoparticles were initially dispersed in CH_2Cl_2, the average hydrodynamic diameter was found to be about 58.2 nm, about 10 times the physical core size of individual nanoparticles (5.0 nm, as determined by TEM measurements). This may be ascribed to the amphiphilic nature of the particles that self-assembled to minimize the exposure of the hydrophilic face to the solvent, as observed previously.[17] It is interesting that with the addition of only a small amount of water (o/w ratio 1:0.06) the size of the nanoparticle ensembles increased significantly to ca. 148.4 nm after mechanical agitation. As shown above in the optical images (Figure 1D), a homogeneous solution was formed with water dispersed into the CH_2Cl_2 solution of AuC6-MPD Janus nanoparticles, likely in the form of reverse micelle-like multilayer vesicle structures with water droplets trapped in the cores. In the case where an oil-in-water dispersion was formed with a large excess of water added to a CH_2Cl_2 solution of AuC6-MPD Janus nanoparticles (o/w ratio 0.06:1, Figure 1A), the average hydrodynamic diameter of the resulting nanoparticle assemblies was found to be even larger at ca. 302.8 nm. This is consistent with the formation of micelle-like superparticulate structures with CH_2Cl_2 droplets as the anchoring cores. The results are summarized in Table 1.

These observations clearly showed the amphiphilicity of Janus nanoparticles that might form (reverse) micelle-like superparticulate structures (Scheme 1). Under the oil-in-water condition (panel A), AuC6-MPD Janus nanoparticles self-assembled into a structure that was analogous to multilayer vesicles, with the hydroxyl-terminated MPD hemispheres situated on the outermost surface and hydrophobic oil (CH_2Cl_2) trapped within the central cores. On the contrary, in the water-in-oil condition (panel B), an opposite orientation was mostly likely formed where the outermost surface of the nanoparticle ensembles would be the hydrophobic hexanethiolate hemispheres and water encapsulated in the ensemble cores.

UV–vis measurements were also carried out to provide further insight into the amphiphilic character of these Janus nanoparticles and the formation of aggregates in different media. The optical absorption profiles of AuC6 (black curve) and AuC6-MPD Janus (red curve) nanoparticles in CH_2Cl_2 were depicted as Figure 2. It can be seen that the original AuC6 nanoparticles (black curve) exhibited an exponential decay profile (Mie scattering) with an absorption peak at 556 nm, characteristic of the surface plasmon resonance of nanosized gold particles.[23,33,34] For the AuC6-MPD Janus nanoparticles (red curve), the surface plasmon peak was broadened and red-shifted to 612 nm, suggesting enhanced interparticle electronic coupling as a consequence of the formation of nanoparticle aggregates, as observed in the above DLS measurements. More interestingly, when a small amount of water was added to the

dx.doi.org/10.1021/la5011506 | Langmuir 2014, 30, 6389–6397

Scheme 1. Schematic Structures of (A) Oil-in-Water and (B) Water-in-Oil Vesicles Formed by Janus Nanoparticles

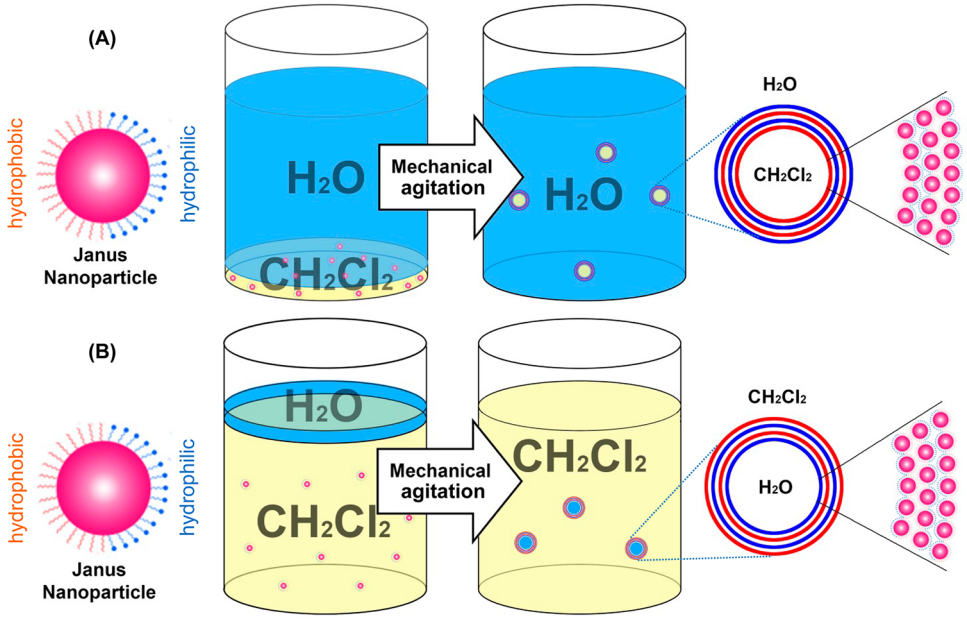

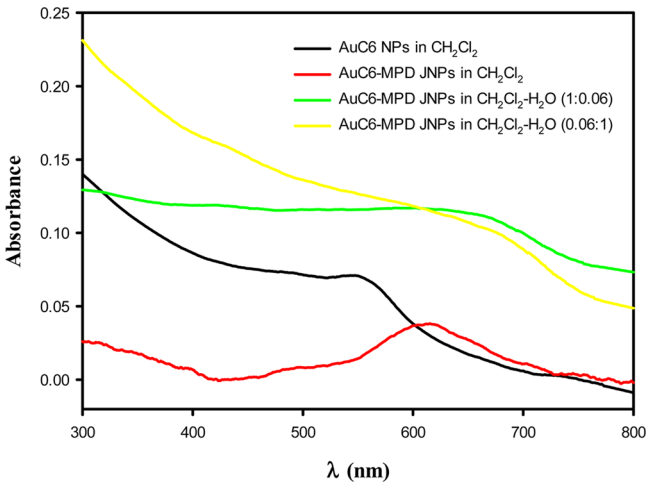

Figure 2. UV−vis absorption spectra of AuC6 NPs in CH_2Cl_2 (black curve) and AuC6-MPD JNPs in CH_2Cl_2 (red curve), in CH_2Cl_2−H_2O (1:0.06, green curve), and in CH_2Cl_2−H_2O (0.06:1, yellow curve).

Janus nanoparticle solution in CH_2Cl_2 (o/w ratio 1:0.06, Figure 1D), the corresponding surface plasmon peak became increasingly broadened and red-shifted to 651 nm (green curve). A more drastic red shift to 668 nm (yellow curve) can be seen when a large excess of water was added to the Janus nanoparticle solution in CH_2Cl_2 (o/w ratio 0.06:1, Figure 1A). These observations are in excellent agreement with the DLS results where larger nanoparticle aggregates were formed in the latter (Table 1).

Taken together, these studies highlight the amphiphilic character of Janus nanoparticles where oil-in-water or water-in-oil vesiclelike superstructures can be readily formed, akin to conventional surfactant molecules, depending on the solvent media. Such unique properties may be exploited for the phase transfer of a diverse variety of guest nanoparticles between the organic and aqueous phases, as manifested below.

Transfer of Hydrophobic Nanoparticles from the Organic to Aqueous Phase. In the first tests, hydrophobic hexanethiolate-protected silver (AgC6) nanoparticles and fullerene (C_{60}) were employed as examples to manifest the phase-transfer properties of Janus nanoparticles from organic to aqueous media. AgC6 and C_{60} were initially dispersed in CH_2Cl_2. With the addition of a large excess of water (o/w ratio 0.06:1), a homogeneous solution was formed when aided by Janus nanoparticles, as depicted in Figure 3A,C, respectively. Yet in the absence of Janus nanoparticles, AgC6 and C_{60} remained at the bottom of the vials, as manifested by the dark-brown CH_2Cl_2 droplets in panels B and D, respectively.

Consistent results were obtained for DLS measurements (Table 1). For the solution of Figure 3A, the average hydrodynamic diameter of the resulting nanoparticle aggregates is ca. 179.9 nm, suggesting that the AgC6 nanoparticles were most likely encapsulated in the CH_2Cl_2 cores as well as between the Janus nanoparticles in the vesicle layers. For the solution of Figure 3C, even larger nanoparticle aggregates were formed with an average hydrodynamic diameter of 274.5 nm due to the formation of C_{60} crystals within the Janus nanoparticle vesicles (vide infra).

The transfer of hydrophobic AgC6 nanoparticles and C_{60} from CH_2Cl_2 to water by AuC6-MPD Janus nanoparticles was further confirmed by UV−vis absorption measurements, as shown in Figure 4. The characteristic surface plasmon resonance of AgC6 nanoparticles in CH_2Cl_2 can be found at 424 nm (Figure 4A, red curve),[35] and with the addition of AuC6-MPD Janus nanoparticles, two absorption bands (green curve) appear at 424 and 556 nm. Note that the latter is consistent with the optical absorption of AuC6-MPD Janus nanoparticles (black curve). The fact that no additional absorption peak emerges indicates no intimate interactions between the two nanoparticles. However, with the addition of a large excess of water (Figure 3A), the UV−vis absorption file became largely featureless with a weak, broad bump between 600 and 800 nm (yellow curve). This is in good agreement with the formation of nanoparticle aggregates such that the surface plasmon resonances were markedly broadened because of enhanced electronic coupling between adjacent gold and silver

dx.doi.org/10.1021/la5011506 | Langmuir 2014, 30, 6389−6397

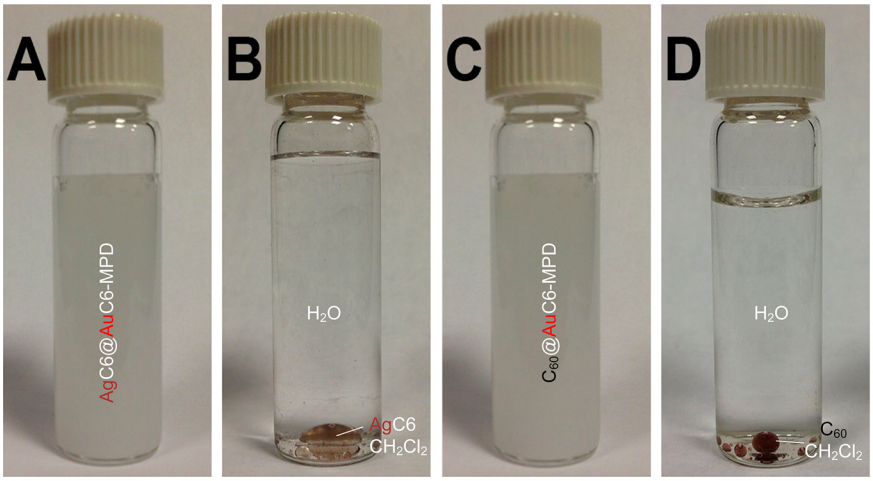

Figure 3. Photographs of 0.05 mg of AgC6 NPs in 300 μL of CH_2Cl_2 mixed with 5 mL of water (A) with and (B) without 0.05 mg of AuC6-MPD Janus nanoparticles and 0.05 mg of fullerene C_{60} in 300 μL of CH_2Cl_2 mixed with 5 mL of water (C) with and (D) without 0.05 mg of AuC6-MPD Janus nanoparticles.

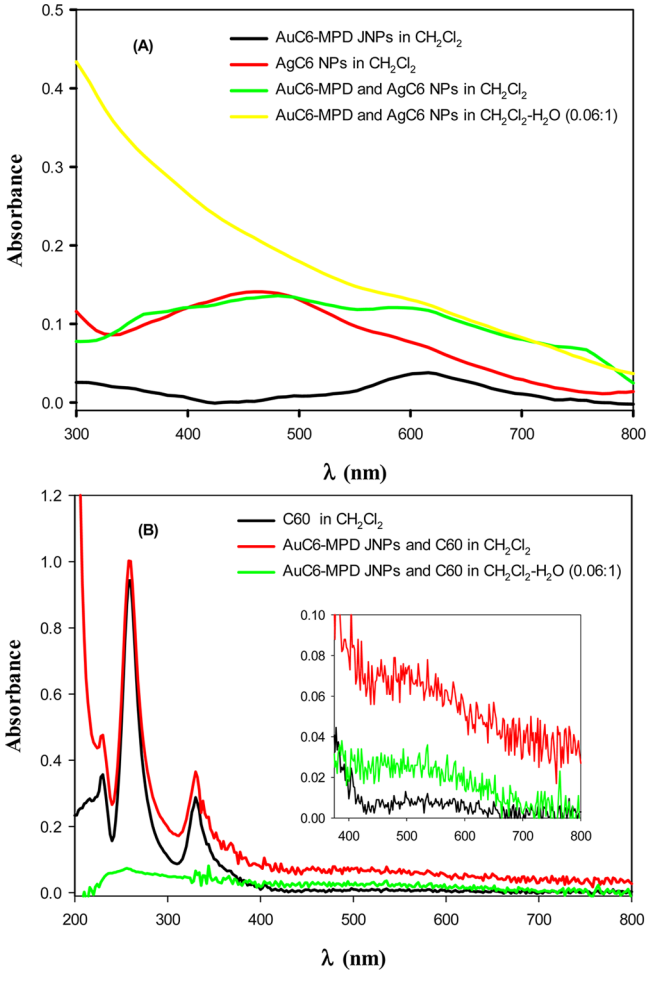

Figure 4. UV−vis adsorption spectra of (A) AgC6 NPs and (B) C_{60} before and after phase transfer from CH_2Cl_2 to water by AuC6-MPD Janus nanoparticles. The inset of panel B is an enlarged image of the absorption profiles between 400 and 800 nm.

nanoparticles, in agreement with results from the aforementioned DLS measurements (Table 1).

The UV−vis spectra of C_{60} before and after phase transfer by Janus nanoparticles are depicted in Figure 4B. For C_{60}

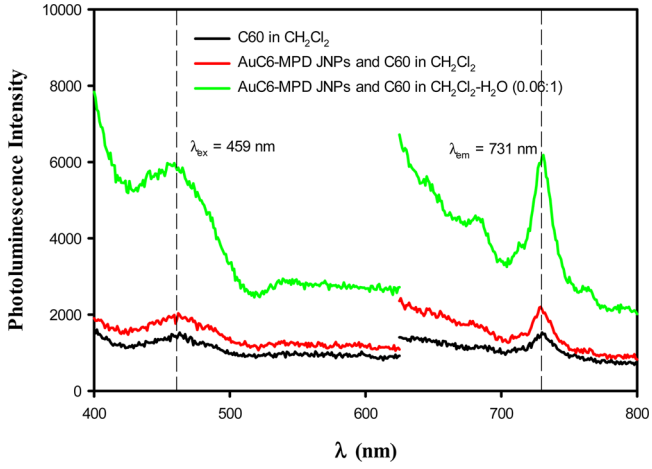

Figure 5. Excitation and emission spectra of C_{60} in CH_2Cl_2 (black curve), mixed with AuC6-MPD JNPs in CH_2Cl_2 (red curve) and after being transferred to water by AuC6-MPD JNPs (green curve).

dispersed in CH_2Cl_2 (black curve), three absorption peaks can be clearly seen at 208, 256, and 328 nm, which may be ascribed to the $8^1T_{1u} \leftarrow 1^1A_g$, $6^1T_{1u} \leftarrow 1^1A_g$, and $3^1T_{1u} \leftarrow 1^1A_g$ transitions of C_{60} molecules, respectively.[36] The same spectral features can be seen with the addition of Janus nanoparticles to the C_{60} solution, along with the emergence of a broad peak within the range of 500 to 600 nm that is due to the gold Janus nanoparticles (red curve and figure inset). However, when C_{60} was transferred to the aqueous phase by the Janus nanoparticles (Figure 3C), the three absorption peaks of C_{60} virtually vanished (green curve), signifying the formation of C_{60} clusters,[25] and the weak, broad band centered at ca. 575 nm (figure inset) may be ascribed to the formation of ensembles of C_{60} and Janus nanoparticles. Note that as C_{60} is barely soluble in water, they are most likely concentrated within the vesicles formed by the Janus nanoparticles in the form of nanocrystals rather than individual molecules of C_{60} (vide infra).

Consistent results were obtained in photoluminescence measurements. As shown in Figure 5, C_{60} exhibits a characteristic reddish orange emission peak at 730 nm (and a corresponding excitation peak at 459 nm, black curves), which was attributed to the triplet state of C_{60} in solutions[37−39] and

dx.doi.org/10.1021/la5011506 | Langmuir 2014, 30, 6389−6397

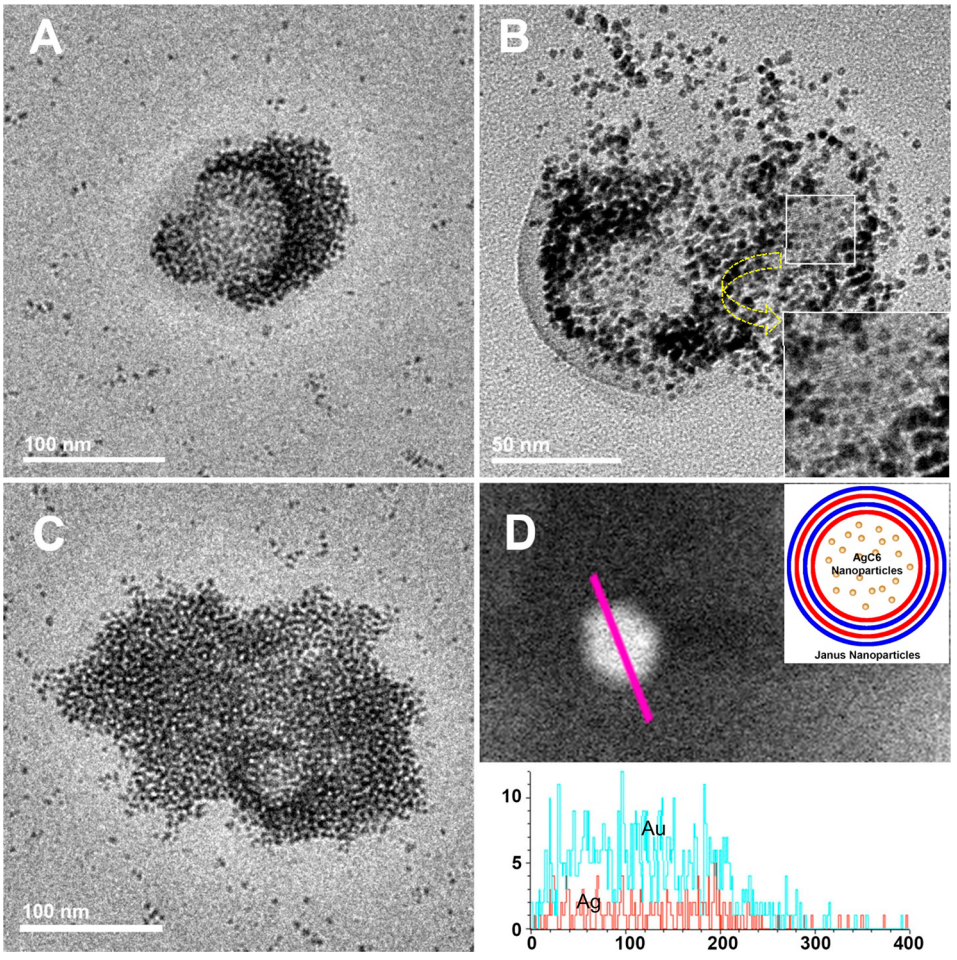

Figure 6. Representative TEM images of (A) AuC6-MPD JNPs alone in CH_2Cl_2–H_2O (o/w ratio 0.06:1), (B) with C_{60} (inset shows crystal lattices of C_{60} nanocrystals), and (C) with AgC6 NPs. (D) Representative STEM image of an aggregate formed with AgC6 and AuC6-MPD JNPs. The top inset is a schematic of the AgC6 nanoparticles encapsulated within the vesicles of AuC6-MPD Janus nanoparticles, and the bottom inset shows the corresponding line scans of EDX elemental mapping with the orange curve for Ag and aqua blue curve for Au.

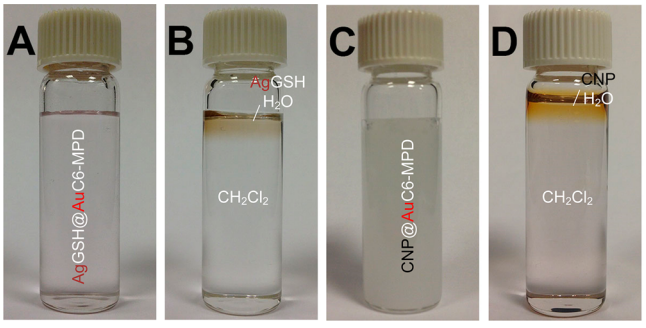

Figure 7. Photographs of 0.05 mg of AgGSH NPs in 300 μL of water mixed with 5 mL of CH_2Cl_2 (A) with and (B) without 0.05 mg of AuC6-MPD JNPs and 0.05 mg of carbon NPs in 300 μL of water mixed with 5 mL of CH_2Cl_2 (C) with and (D) without 0.05 mg of AuC6-MPD JNPs.

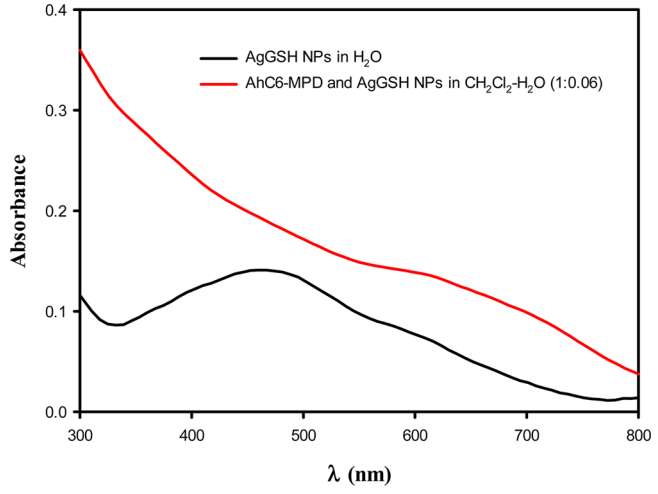

Figure 8. UV–vis adsorption spectra of AgGSH NPs in aqueous solution (black curve) and after being transferred to CH_2Cl_2 by AuC6-MPD JNPs (red curve).

thin films.[40,41] Note that the photoluminescence profiles showed no obvious variation by mixing AuC6-MPD Janus nanoparticles with C_{60} in CH_2Cl_2 (red curves), which suggests no strong interactions between C_{60} and AuC6-MPD Janus nanoparticles in CH_2Cl_2. However, the peak intensity increased markedly with the addition of a large excess of water (green curves), indicating an enhanced local concentration of C_{60} in the solution, which is consistent with results from UV–vis measurements in which C_{60} was encapsulated within the CH_2Cl_2 cores of the Janus nanoparticle vesicles.

The formation of superparticulate ensembles can also be visualized by TEM measurements. Figure 6A depicts a

dx.doi.org/10.1021/la5011506 | Langmuir 2014, 30, 6389–6397

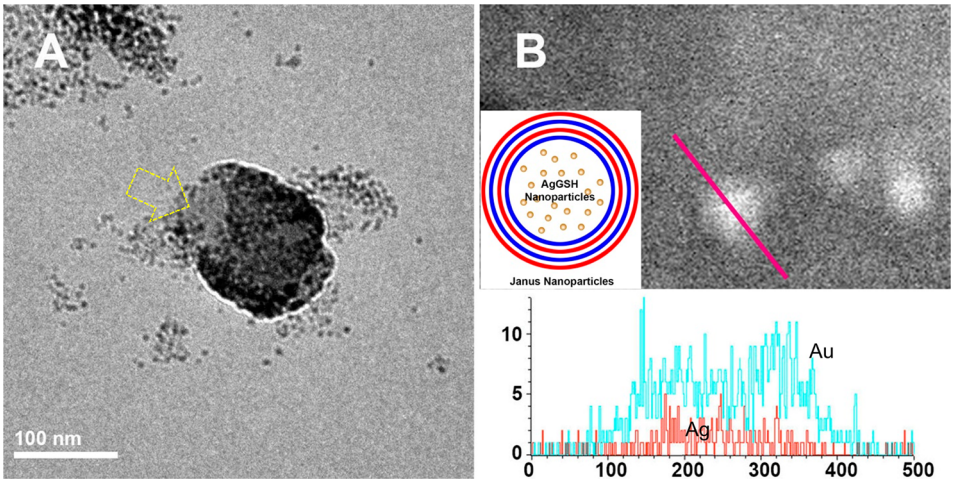

Figure 9. TEM (A) and STEM (B) images of the aggregate formed with AgGSH NPs and AuC6-MPD JNPs. In panel B, the top inset is a schematic of the AgGSH nanoparticles encapsulated within the vesicles of AuC6-MPD Janus nanoparticles, and the bottom inset is the line scan of EDX elemental analysis of a representative nanoparticle ensemble, with the aqua blue curve for gold and the orange curve for silver.

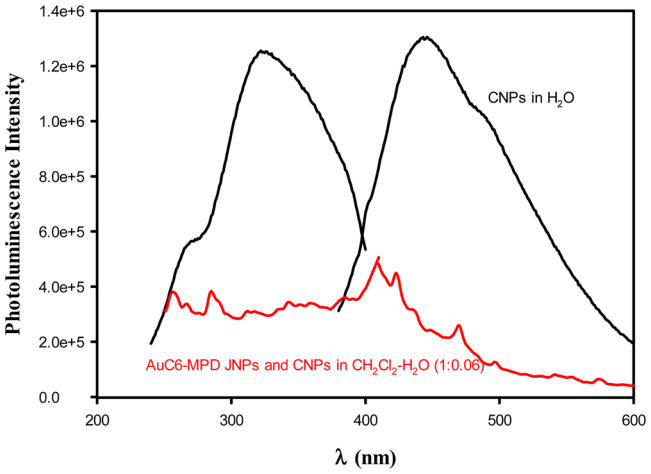

Figure 10. Excitation and emission spectra of CNPs in water (black curve) and after being transferred to CH_2Cl_2 with AuC6-MPD JNPs (red curve).

representative TEM micrograph of the AuC6-MPD Janus particles in CH_2Cl_2–H_2O (o/w ratio 0.06:1, Figure 1A), where one can see a largely vesiclelike structure of about 160 nm in diameter constituting multiple layers of nanoparticles that encapsulated an empty core. This again suggests the amphiphilicity of the Janus nanoparticles that self-assembled into a vesiclelike superstructure. In the phase transfer of C_{60} from CH_2Cl_2 to water (Figure 3C), one can see from Figure 6B that C_{60} molecules, represented by the light-contrast objects, largely clustered together to form nanoscale crystals that were trapped within the AuC6-MPD Janus nanoparticle ensembles, as highlighted by the white square. Furthermore, the fringe spacing of the C_{60} nanocrystals was estimated to be 0.50 nm, which is consistent with the (220) planes (0.50074 nm) of face-centered cubic (fcc) C_{60} crystals.[42,43] For the transfer of AgC6 nanoparticles (Figure 3A), a vesiclelike structure can also be found, yet with a marked shrinkage of the void space in the center, as shown in Figure 6C. This is likely due to the encapsulation of the AgC6 nanoparticles in the CH_2Cl_2 cores of the Janus nanoparticle vesicles (top inset to panel D). In fact, line scans based on the EDX elemental analysis of a typical nanoparticle ensemble showed that the Ag profile (orange curve) was mostly enclosed within the Au signals (blue curve), as depicted in Figure 6D and bottom inset.

Transfer of Hydrophilic Nanoparticles from the Water Phase to the Organic Phase. In this study, water-soluble glutathione-stabilized silver (AgGSH) and carbon (CNP) nanoparticles were used as examples of phase transfer from water to CH_2Cl_2 by AuC6-MPD Janus nanoparticles. As illustrated in Figure 7, homogeneous solutions were obtained when a large excess of CH_2Cl_2 was added to the AgGSH or CNP solutions in a small amount of water (o/w ratio 1:0.06) in the presence of AuC6-MPD Janus nanoparticles, as depicted in panels A and C, respectively. In contrast, in the absence of Janus nanoparticles, the water phase remained clearly separated from CH_2Cl_2, as manifested by the brown layers on the CH_2Cl_2 surface in panels B and D.

The dimensions of the nanoparticle ensembles were then determined by DLS measurements (Table 1). For solution A, where water-soluble AgGSH nanoparticles were transferred to CH_2Cl_2 by AuC6-MPD Janus nanoparticles, the average hydrodynamic diameter of stable aggregates was found to be 279.9 nm, about 125 times larger than that of the AgGSH nanoparticles alone in water (2.2 nm). For solution C, where CNPs were transferred to CH_2Cl_2 with AuC6-MPD Janus nanoparticles, the size of the nanoparticle ensembles was determined to be 426.3 nm, in comparison to 7.4 nm for individual CNPs in water.

The corresponding UV–vis absorption spectra are shown in Figure 8. For AgGSH nanoparticles alone in water, the surface plasmon resonance peak can be identified at 454 nm (black curve), characteristic of nanosized silver particles.[35] After being transferred to the CH_2Cl_2 phase by the AuC6-MPD Janus nanoparticles (o/w ratio 1:0.06), the absorption profile was largely featureless with a broad peak within the range of 550 to 800 nm. The broadening and red shift of the surface plasmon resonance again arose from strong electronic interactions between the nanoparticles as a result of the formation of nanoparticle aggregates (red curve).

The formation of nanoparticle aggregates can also be clearly seen in TEM measurements. Figure 9A depicts a representative nanoparticle ensemble with a roughly spherical shape of about 160 nm in diameter, similar to those of AgC6 and AuC6-MPD Janus nanoparticles in CH_2Cl_2–H_2O (Figure 6C). The vesicle-

dx.doi.org/10.1021/la5011506 | *Langmuir* 2014, 30, 6389–6397

like structure is evidenced by the partial collapse of the ensemble, as highlighted by the yellow arrow in panel A. Line scans based on the EDX elemental analysis of a typical nanoparticle ensemble in panel B showed that indeed the silver signals (orange curve) were enclosed within the gold profile (blue curve), as manifested in the bottom inset. This is consistent with the encapsulation of AgGSH nanoparticles within the Janus nanoparticle vesicles (top inset).

For carbon nanoparticles, the effective transfer from water to the organic phase can also be seen in optical measurements. From the excitation and emission photoluminescence spectra in Figure 10, one can see that carbon nanoparticles in water (black curves) exhibited a well-defined excitation peak at 322 nm and a corresponding emission peak at 444 nm, which have been ascribed to electronic transitions of phenanthrenequinone-like moieties on the nanoparticle surface.[31,32] In contrast, when the carbon nanoparticles were transferred to the CH_2Cl_2 phase by the Janus nanoparticles, the photoluminescence was substantially quenched (red curves). This quenching may be accounted for by the close proximity of gold nanoparticles to the carbon nanoparticles where metal nanoparticles are known to be effective luminescence quenchers.[44]

CONCLUSIONS

The amphiphilicity of Janus nanoparticles was tested by a series of experiments. With hydrophobic capping ligands on one hemisphere and hydrophilic ones on the other, Janus nanoparticles were readily dispersed in both water and organic media and formed oil-in-water micelle-like or water-in-oil reverse micelle-like superparticulate structures by mechanical agitation. This unique property was exploited for the transfer of hydrophobic nanoparticles (e.g., AgC6 and C_{60} nanoparticles) from CH_2Cl_2 to water as well as for the transfer of water-soluble AgGSH and carbon nanoparticles from water to CH_2Cl_2, in sharp contrast to the homogeneously capped AuC6 nanoparticles. In these tests, the formation of vesicle-like nanoparticle ensembles was clearly visualized in TEM measurements, with the shells consisting of multiple layers of Janus nanoparticles and guest nanoparticles encapsulated primarily in the cores. Consistent results were obtained in DLS, UV−vis, and photoluminescence measurements. The studies further highlight the analogous behaviors of Janus nanoparticles with respect to conventional surfactant molecules in the formation of (reverse) micelle-like structures and their application as a unique phase-transfer catalyst in the formation of functional nanocomposites.

AUTHOR INFORMATION

Corresponding Author

*E-mail: shaowei@ucsc.edu.

Author Contributions

The manuscript was written through contributions of all authors. All authors have given approval to the final version of the manuscript.

Notes

The authors declare no competing financial interest.

ACKNOWLEDGMENTS

This work was supported, in part, by the National Science Foundation (CHE − 1012258 and CHE − 1265635). TEM studies were carried out at the National Center for Electron Microscopy, Lawrence Berkeley National Laboratory, which is supported by the Department of Energy, as part of a user project.

REFERENCES

(1) Song, Y.; Chen, S. W. Janus Nanoparticles: Preparation, Characterization, and Applications. *Chem.—Asian J.* **2014**, *9*, 418−430.
(2) Kim, S. H.; Lee, S. Y.; Yang, S. M. Janus Microspheres for a Highly Flexible and Impregnable Water-Repelling Interface. *Angew. Chem., Int. Ed.* **2010**, *49*, 2535−2538.
(3) Synytska, A.; Khanum, R.; Ionov, L.; Cherif, C.; Bellmann, C. Water-Repellent Textile via Decorating Fibers with Amphiphilic Janus Particles. *ACS Appl. Mater. Interfaces* **2011**, *3*, 1216−1220.
(4) McConnell, M. D.; Kraeutler, M. J.; Yang, S.; Composto, R. J. Patchy and Multiregion Janus Particles with Tunable Optical Properties. *Nano Lett.* **2010**, *10*, 603−609.
(5) Shaviv, E.; Schubert, O.; Alves-Santos, M.; Goldoni, G.; Felice, R. D.; Valleé, F.; Fatti, N.; Banin, D. U.; Soñnichsen, C. Absorption Properties of Metal−Semiconductor Hybrid Nanoparticles. *ACS Nano* **2011**, *5*, 4712−4719.
(6) Fernández-Rodríguez, M. A.; Rodríguez-Valverde, M. A.; Cabrerizo-Vílchez, M.; Hidalgo-Alvarez, R. Surface Activity and Collective Behaviour of Colloidally Stable Janus-Like Particles at the Air−Water Interface. *Soft Matter* **2014**, *10*, 3471−3476.
(7) Smoukov, S. K.; Gangwal, S.; Marquez, M.; Velev, O. D. Reconfigurable Responsive Structures Assembled from Magnetic Janus Particles. *Soft Matter* **2009**, *5*, 1285−1292.
(8) Ren, B.; Ruditskiy, A.; Song, J. H.; Kretzschmar, I. Assembly Behavior of Iron Oxide-Capped Janus Particles in a Magnetic Field. *Langmuir* **2012**, *28*, 1149−1156.
(9) Kim, S. H.; Sim, J. Y.; Lim, J. M.; Yang, S. M. Magnetoresponsive Microparticles with Nanoscopic Surface Structures for Remote-Controlled Locomotion. *Angew. Chem., Int. Ed.* **2010**, *49*, 3786−3790.
(10) Yin, S.; Wang, C.; Yu, Z.; Wang, J. ; Liu, S.-S.; Chen, S. Versatile Bifunctional Magnetic-Fluorescent Responsive Janus Supraballs Towards the Flexible Bead Display. *Adv. Mater.* **2011**, *23*, 2915−2919.
(11) Nisisako, T.; Torii, T.; Takahashi, T.; Takizawa, Y. Synthesis of Monodisperse Bicolored Janus Particles with Electrical Anisotropy Using a Microfluidic Co-Flow System. *Adv. Mater.* **2006**, *18*, 1152−1156.
(12) Perro, A.; Reculusa, S.; Pereira, F.; Delville, M. H.; Mingotaud, C.; Duguet, E.; Bourgeat-Lami, E.; Ravaine, S. Towards Large Amounts of Janus Nanoparticles through a Protection-Deprotection Route. *Chem. Commun.* **2005**, 5542−5543.
(13) Perro, A.; Reculusa, S.; Ravaine, S.; Bourgeat-Lami, E. B.; Duguet, E. Design and Synthesis of Janus Micro- And Nanoparticles. *J. Mater. Chem.* **2005**, *15*, 3745−3760.
(14) Roh, K. H.; Martin, D. C.; Lahann, J. Biphasic Janus Particles with Nanoscale Anisotropy. *Nat. Mater.* **2005**, *4*, 759−763.
(15) Suzuki, D.; Kawaguchi, H. Janus Particles with a Functional Gold Surface for Control of Surface Plasmon Resonance. *Colloid Polym. Sci.* **2006**, *284*, 1471−1476.
(16) Nie, Z.; Li, W.; Seo, M.; Xu, S.; Kumacheva, E. Janus and Ternary Particles Generated by Microfluidic Synthesis: Design, Synthesis, And Self-Assembly. *J. Am. Chem. Soc.* **2006**, *128*, 9408−9412.
(17) Pradhan, S.; Xu, L. P.; Chen, S. W. Janus Nanoparticles by Interfacial Engineering. *Adv. Funct. Mater.* **2007**, *17*, 2385−2392.
(18) Song, Y.; Klivanski, L.; Liu, Y.; Chen, S. W. Enhanced Stability of Janus Nanoparticles by Covalent Crosslinking of Surface Ligands. *Langmuir* **2011**, *27*, 14581−14588.
(19) Xu, L. P.; Pradhan, S.; Chen, S. W. Adhesion Force Studies of Janus Nanoparticles. *Langmuir* **2007**, *23*, 8544−8548.
(20) Pradhan, S.; Brown, L.; Konopelski, J.; Chen, S. W. Janus Nanoparticles: Reaction Dynamics and NOESY Characterization. *J. Nanopart. Res.* **2009**, *11*, 1895−1903.
(21) Pradhan, S.; Ghosh, D.; Chen, S. W. Janus Nanostructures Based on Au-TiO_2 Heterodimers and Their Photocatalytic Activity in the Oxidation of Methanol. *ACS Appl. Mater. Interfaces* **2009**, *1*, 2060−2065.

(22) Xu, Q.; Kang, X. W.; Bogomolni, R. A.; Chen, S. W. Controlled Assembly of Janus Nanoparticles. *Langmuir* **2010**, *26*, 14923−14928.
(23) Underwood, S.; Mulvaney, P. Effect of the Solution Refractive-Index on the Color of Gold Colloids. *Langmuir* **1994**, *10*, 3427−3430.
(24) Sastry, M.; Kumar, A.; Mukherjee, P. Phase Transfer of Aqueous Colloidal Gold Particles into Organic Solutions Containing Fatty Amine Molecules. *Colloids Surf., A* **2001**, *181*, 255−259.
(25) Torres, V. M.; Posa, M.; Srdjenovic, B.; Simplicio, A. L. Solubilization of Fullerene C60 in Micellar Solutions of Different Solubilizers. *Colloids Surf., B* **2011**, *82*, 46−53.
(26) Brauer, G. *Handbook of Preparative Inorganic Chemistry*, 2nd ed.; Academic Press: New York, 1963.
(27) Brust, M.; Walker, M.; Bethell, D.; Schiffrin, D. J.; Whyman, R. Synthesis of Thiol-Derivatized Gold Nanoparticles in a 2-Phase Liquid-Liquid System. *J. Chem. Soc., Chem. Commun.* **1994**, 801−802.
(28) Song, Y.; Liu, K.; Chen, S. W. AgAu Bimetallic Janus Nanoparticles and Their Electrocatalytic Activity for Oxygen Reduction in Alkaline Media. *Langmuir* **2012**, *28*, 17143−17152.
(29) Song, Y.; Chen, S. W. Trimetallic Ag@AuPt Neapolitan Nanoparticles. *Nanoscale* **2013**, *5*, 7284−7289.
(30) Yuan, X.; Tay, Y.; Dou, X.; Luo, Z.; Leong, D. T.; Xie, J. Glutathione-Protected Silver Nanoclusters as Cysteine-Selective Fluorometric and Colorimetric Probe. *Anal. Chem.* **2012**, *85*, 1913−1919.
(31) Tian, L.; Ghosh, D.; Chen, W.; Pradhan, S.; Chang, X. J.; Chen, S. W. Nanosized Carbon Particles from Natural Gas Soot. *Chem. Mater.* **2009**, *21*, 2803−2809.
(32) Tian, L.; Song, Y.; Chang, X. J.; Chen, S. W. Hydrothermally Enhanced Photoluminescence of Carbon Nanoparticles. *Scr. Mater.* **2010**, *62*, 883−886.
(33) Bohren, C. F.; Huffman, D. R.: *Absorption and Scattering of Light by Small Particles*; Wiley: New York, 1983.
(34) Alvarez, M. M.; Khoury, J. T.; Schaaff, T. G.; Shafigullin, M. N.; Vezmar, I.; Whetten, R. L. Optical Absorption Spectra of Nanocrystal Gold Molecules. *J. Phys. Chem. B* **1997**, *101*, 3706−3712.
(35) Creighton, J. A.; Eadon, D. G. Ultraviolet Visible Absorption-Spectra of the Colloidal Metallic Elements. *J. Chem. Soc., Faraday Trans.* **1991**, *87*, 3881−3891.
(36) Leach, S.; Vervloet, M.; Despres, A.; Breheret, E.; Hare, J. P.; Dennis, T. J.; Kroto, H. W.; Taylor, R.; Walton, D. R. M. Electronic Spectra and Transitions of the Fullerene C60. *Chem. Phys.* **1992**, *160*, 451−466.
(37) Sun, Y. P.; Wang, P.; Hamilton, N. B. Fluorescence-Spectra and Quantum Yields of Buckminsterfullerene (C-60) in Room-Temperature Solutions - No Excitation Wavelength Dependence. *J. Am. Chem. Soc.* **1993**, *115*, 6378−6381.
(38) D'Souza, F.; Deviprasad, G. R.; El-Khouly, M. E.; Fujitsuka, M.; Ito, O. Probing the Donor-Acceptor Proximity on the Physicochemical Properties of Porphyrin-Fullerene Dyads: "Tail-on" and "Tail-off" Binding Approach. *J. Am. Chem. Soc.* **2001**, *123*, 5277−5284.
(39) Accorsi, G.; Armaroli, N. Taking Advantage of the Electronic Excited States of [60]-Fullerenes. *J. Phys. Chem. C* **2010**, *114*, 1385−1403.
(40) Faiman, D.; Goren, S.; Katz, E. A.; Koltun, M.; Melnik, N.; Shames, A.; Shtutina, S. Structure and Optical Properties of C60 Thin Films. *Thin Solid Films* **1997**, *295*, 283−286.
(41) Ma, G.; Yang, Y.; Chen, G. Anomalous Photoluminescence from C60 Polymethyl Methacrylate Films. *Mater. Lett.* **1998**, *34*, 377−382.
(42) McCready, D. E.; Alnajjar, M. S. Powder Data for Buckminsterfullerene, C60. *Powder Diffr.* **1994**, *9*, 93−95.
(43) Deguchi, S.; Mukai, S.-a.; Sakaguchi, H.; Nonomura, Y. Non-Engineered Nanoparticles of C60. *Sci. Rep.* **2013**, *3*, 2094−1.
(44) Maxwell, D. J.; Taylor, J. R.; Nie, S. M. Self-Assembled Nanoparticle Probes for Recognition and Detection of Biomolecules. *J. Am. Chem. Soc.* **2002**, *124*, 9606−9612.